Pyruvate uptake is increased in highly invasive ovarian cancer cells under anoikis conditions for anaplerosis, mitochondrial function, and migration

Christine A. Caneba, Nadège Bellance, Lifeng Yang, Lisa Pabst and Deepak Nagrath

Am J Physiol Endocrinol Metab 303:E1036-E1052, 2012. First published 14 August 2012;
doi: 10.1152/ajpendo.00151.2012

Am J Physiol Endocrinol Metab 303: E1036–E1052, 2012.
First published August 14, 2012; doi:10.1152/ajpendo.00151.2012.

Pyruvate uptake is increased in highly invasive ovarian cancer cells under anoikis conditions for anaplerosis, mitochondrial function, and migration

Christine A. Caneba,[1,2] Nadège Bellance,[1,3] Lifeng Yang,[1,3] Lisa Pabst,[1,3] and Deepak Nagrath[1,2,3]

[1]*Laboratory for Systems Biology of Human Diseases, Rice University, Houston, Texas;* [2]*Department of Bioengineering, Rice University, Houston, Texas; and* [3]*Department of Chemical and Biomolecular Engineering, Rice University, Houston, Texas*

Submitted 26 March 2012; accepted in final form 13 August 2012

Caneba CA, Bellance N, Yang L, Pabst L, Nagrath D. Pyruvate uptake is increased in highly invasive ovarian cancer cells under anoikis conditions for anaplerosis, mitochondrial function, and migration. *Am J Physiol Endocrinol Metab* 303: E1036–E1052, 2012. First published August 14, 2012; doi:10.1152/ajpendo.00151.2012.—Anoikis resistance, or the ability for cells to live detached from the extracellular matrix, is a property of epithelial cancers. The "Warburg effect," or the preference of cancer cells for glycolysis for their energy production even in the presence of oxygen, has been shown to be evident in various tumors. Since a cancer cell's metastatic ability depends on microenvironmental conditions (nutrients, stromal cells, and vascularization) and is highly variable for different organs, their cellular metabolic fluxes and nutrient demand may show considerable differences. Moreover, a cancer cell's metastatic ability, which is dependent on the stage of cancer, may further create metabolic alterations depending on its microenvironment. Although recent studies have aimed to elucidate cancer cell metabolism under detached conditions, the nutrient demand and metabolic activity of cancer cells under nonadherent conditions remain poorly understood. Additionally, less is known about metabolic alterations in ovarian cancer cells with varying invasive capability under anoikis conditions. We hypothesized that the metabolism of highly invasive ovarian cancer cells in detachment would differ from less invasive ovarian cancer cells and that ovarian cancer cells will have altered metabolism in detached vs. attached conditions. To assess these metabolic differences, we integrated a secretomics-based metabolic footprinting (MFP) approach with mitochondrial bioenergetics. Interestingly, MFP revealed higher pyruvate uptake and oxygen consumption in more invasive ovarian cancer cells than their less invasive counterparts. Furthermore, ATP production was higher in more invasive vs. less invasive ovarian cancer cells in detachment. We found that pyruvate has an effect on highly invasive ovarian cancer cells' migration ability. Our results are the first to demonstrate that higher mitochondrial activity is related to higher ovarian cancer invasiveness under detached conditions. Importantly, our results bring insights regarding the metabolism of cancer cells under nonadherent conditions and could lead to the development of therapies for modulating cancer cell invasiveness.

oxidative phosphorylation; metabolomics; Warburg effect; bioenergetics; cancer migration and anoikis

OVARIAN CANCER REMAINS A LEADING CAUSE of gynecological malignancy-related deaths and is often detected in the late stages, when the cancer has already metastasized (5). Of all ovarian cancer diagnoses, most are classified as epithelial ovarian carcinoma (17). In the process of epithelial ovarian cancer metastasis, cancer cells can remain viable while they are suspended in peritoneal fluid in the peritoneal cavity. A normal epithelial cell would in this environment undergo anoikis or epithelial cell death due to detachment, first coined by Frisch and Francis (8) in 1994. However, cancer cells, including ovarian cancer cells, can survive without extracellular matrix attachment and are thus considered anoikis resistant. Anoikis resistance in cancer has been widely studied from the genetics perspective. Various genes and proteins, including Zeb1 (32), mammalian target of rapamycin (mTOR) (33), and yes-associated protein in prostate cancer (43), have been observed to play a role in anoikis resistance.

In the 1920s, Otto Warburg first made the observation that cancer cells had higher rates of glycolysis than normal cells (35). This phenomenon is now known as the "Warburg effect" and has been observed in various types of cancers, including ovarian cancer (14). For example, 2-deoxy-D-glucose, a glucose analog, has been shown to be effective as an anticancer treatment in several cancers, including ovarian cancer in vitro (42). Warburg's finding sparked interest in research in cancer metabolism from the protein and genetic perspective. c-Myc and hypoxia-inducible factor-1 (HIF-1) have been shown recently, through Western blot and lactate production analysis, to play a role in increased glycolysis in early passage breast cancer cells. Pyruvate kinase M2 has been shown to be a regulator of glycolysis in cancer cells (22), in addition to being regulated by epidermal growth factor (EGF) receptor in glioblastoma (37), and by mTOR (33). mTOR has also been found recently to interact with lactate dehydrogenase kinase B in cancer cells (40).

The metabolic changes that are linked to anoikis resistance and the proteins and genes responsible for this remodeling are currently under investigation. Recently, the effect of oncogene ErbB2 on glucose uptake and ATP production in detachment (29) and EGF stability (12) have been investigated in mammary carcinoma MCF-10A cells (12, 29). Furthermore, ErbB2 expression has been found to affect glycolytic protein pyruvate dehydrogenase and pyruvate dehydrogenase kinase-4 in these mammary carcinoma cells cultured in detachment (11). More specifically, when MCF-10A cells are cultured in detachment, glucose and glutamine uptake decreased and tricarboxylic acid (TCA) cycle and glycolysis rate decreased compared with in adherent conditions for this breast cancer cell line (11). However, the role of metabolism in anoikis resistance of ovarian cancer cells and the differences in metabolism between highly invasive vs. less invasive ovarian cancer cells remain to be studied. Importantly, the generalization of cancer metabolic profiling results for cancer cells originating from different organs can be restrictive because of the variable metabolic state of cancer cells due to exogenous factors, including hormonal dependency, microenvironmental conditions, and considerable differences in nutrient consumption/uptake.

We hypothesized that metabolism of highly invasive ovarian cancer cells would contrast with the less invasive ovarian cancer cells and that ovarian cancer cells have remodeling of

Address for reprint requests and other correspondence: D. Nagrath, Dept. of Chemical and Biomolecular Engineering, Rice University, MS-362 Abercrombie Bldg., 6100 Main St., Houston, TX 77251-1892, (e-mail: deepak.nagrath@rice.edu).

metabolism when they are cultured in detachment as opposed to attachment. Recently, more invasive ovarian cells (SKOV3) were shown to have more elevated monoacylglycerol lipase activity than less invasive ovarian cells (OVCAR3) (24). Here, we used metabolic footprinting (MFP) coupled with bioenergetics analysis to investigate the metabolic differences between more invasive and less invasive ovarian cancer cells under both attached and detached conditions (4a, 22a, 22b). Furthermore, we hypothesized that these differences in metabolism would have an effect on cell migration. Our observations are the first to demonstrate that oxygen consumption rate (OCR) was considerably higher in more invasive ovarian cancer cells (SKOV3ip1) than less invasive ovarian cancer cells (OVCAR3) in nonadherent conditions. Interestingly, we found that pyruvate uptake was significantly higher for the highly invasive ovarian cancer cells compared with the less invasive ovarian cancer cells under detached and attached conditions, indicating that pyruvate may be driving a higher TCA cycle flux and the oxidative phosphorylation rate in the more invasive ovarian cancer cells. ATP production was also higher in more invasive ovarian cancer cells vs. less invasive ovarian cancer cells, which indicates that higher TCA cycle flux and oxidative phosphorylation may have resulted in higher ATP production. Finally, we conclude that pyruvate has an effect on migration in attached ovarian cancer cells. Our results derived from our integrated MFP- and bioenergetics-based approach demonstrate for the first time the importance of pyruvate and mitochondrial metabolism in migration and alterations of metabolism in ovarian cancer cells with variable metastatic abilities.

MATERIALS AND METHODS

Cells and reagents. Ovarian cancer cells OVCAR3 and SKOV3 were purchased from ATCC on behalf of Rice University. SKOV3ip1 cells were kindly provided by Dr. Anil Sood of MD Anderson Cancer Center. Cells were grown in RPMI containing 10% fetal bovine serum. Cells used in these experiments were cultured below 75 passages.

Two-dimensional anchorage-independent experiments. For a two-dimensional poly(2-hydroxymethacrylate) (Poly-HEMA) culture, each well of a 12-well plate was coated two times with 500 μl of 12 mg/ml Poly-HEMA solution (Sigma-Aldrich) in a tissue culture hood. Plates were then allowed 1–2 days to dry at room temperature. Wells were washed twice with 1× PBS before use. OVCAR3, SKOV3, and SKOV3ip1 cells that were ≈80% confluent in flasks were seeded at certain densities in a 12-well plate to obtain ≥50% confluence in wells and to avoid overconfluence in the wells. For 12-well plates, seeding density was determined to be 150,000 cells/well for 24-h culture and 90,000 cells/well for 48-h culture. These plates were either uncoated or coated with Poly-HEMA. Similarly, cells were also seeded in six-well low-attachment plates (Corning) or uncoated six-well plates at densities of 300,000 cells/well for 24-h culture and 150,000 cells/well for 48-h culture.

Matrigel culture. Matrigel culture protocol was based on that from Dr. Joan S. Brugge's laboratory at Harvard University, Boston, MA. Briefly, eight-well chamber slides (Millipore) were chilled and coated with 45 μl/well of Matrigel (BD Biosciences). The coated slides were then incubated with 5% carbon dioxide ≥30 min prior to seeding. Cells were then trypsinized and seeded at 6,000 cells/well in 400 μl of medium containing 2% Matrigel. Medium was changed every other day, and cells were harvested on *days 6* and *12* of culture.

Cell viability. Cell viability was first determined using the LIVE/DEAD Viability/Cytotoxicity Kit for Mammalian Cells (L3224) based on the manufacturer's protocol. Briefly, cells were seeded at 90,000 cells/well in a 12-well plate coated with Poly-HEMA. After 48 h, cells and media were collected, centrifuged, and washed with 1 ml of PBS. Two-hundred microliters of each cell suspension was incubated for 45 min in the dark with 200 μl of cell death staining solution (PBS solution with 2 μM calcein AM and 5 μM ethidium bromide) on a microscope coverslip. Finally, 10 μl of cell death staining solution was added to microscope slide, and a coverslip was inverted onto the slide and imaged.

Cell viability was also quantified using trypan blue exclusion assay for nonadherent cells, as described previously (6). Briefly, cells were seeded at 90,000 cells/well in a 12-well plate coated with Poly-HEMA and noncoated plates. Cells were incubated for 48 h and then harvested. After medium was removed, cells were exposed for 5 min to trypsin (0.05%) to remove clumps. Equal parts cell suspension and trypan blue were then mixed, and live and dead cells were counted on a hemocytometer. At least nine fields of view from each well were analyzed.

For pyruvate cell viability, cells were seeded at 45,000 cells/well in 12-well plates and incubated for 3 days in medium originally containing 0, 1, and 10 mM pyruvate. Cell viability was then assessed using trypan blue exclusion assay, as described above.

Matrigel invasion assay. Invasion assays were conducted using BD Matrigel culture inserts. Briefly, 24-well 8.0-μm pore size polyethylene terephthalate membrane inserts (BD Biosciences) were washed twice with RPMI medium and then coated with 20 μl of reduced growth factor Matrigel (1:6 dilution; BD Biosciences) and incubated for 30 min in a 5% CO_2 incubator for gel formation. Ovarian cancer cells (OVCAR3, SKOV3, SKOV3 ip) were trypsinized, and 100,000 cells in 200 μl of fresh medium were plated into the upper chamber. Next, 300 μl of medium was added to the lower chamber, and the plate was incubated for 24 h. After incubation, medium in the lower chamber was aspirated, and invaded cells were treated with 5% glutaraldehyde in PBS for 10 min to fix the cells and then washed in PBS solution three times. Next, 0.5% toluidine blue in 2% sodium carbonate was added to cells for 20 min at room temperature. Subsequently, inserts were washed three times in PBS solution. The noninvaded cells on the inner surface of upper chambers were carefully wiped by using a cotton swab. Finally, invaded cells were counted under ×20 magnification for at least three fields per insert.

Metabolic assays. Glucose consumption assay was performed using Wako Glucose kit according to the manufacturer's protocol. Briefly, a 2-μl sample and 250 μl of reconstituted Wako glucose reagent was added to a 96-well assay plate and incubated while shaking at 37°C for 5 min. The change in absorbance, indicating the presence of glucose, was measured at 505 nm by using a spectrophotometer (SpectraMax M5; Molecular Devices).

Lactate secretion was determined using the Trinity Lactate Kit according to manufacturer's protocol. Briefly, lactate reagent was reconstituted with 10 ml of milliohm water and diluted 1:4 in 0.1 M Tris solution (pH = 7.0). Media samples were diluted 1:10 in PBS, and lactate reagent was added to the diluted samples in an assay plate. The plate was protected from light and incubated for 1 h before the change in absorbance was read on a spectrophotometer at 540 nm.

The pyruvate assay used measures the amount of sodium dehydrogenase (NADH) oxidized, which correlates with the amount of pyruvate in the samples. Pyruvate uptake analysis was performed using the following protocol. Briefly, NADH solution was created by reconstituting NADH powder (Sigma-Aldrich) in 50 ml of Tris solution (pH = 7.0). Lactate dehydrogenase was reconstituted in 50% glycerol and diluted 1:20 in Tris solution (pH = 7.0). In a 96-well plate, 20 μl of sample was added to each well along with the NADH reagent. A prereading was taken at 340 nm in a spectrophotometer, and lactate dehydrogenase was added to the wells. Plate was incubated for 1 h without carbon dioxide, and subsequent measurements were taken on a spectrophotometer.

ATP measurements. To measure ATP production, a bioluminescent Cell Titer-Glo Kit (Promega) was used. Half of two 96-well plates

(white with clear bottom) were coated first with 84 μl of 12 $mg \cdot ml^{-1} \cdot well^{-1}$ Poly-HEMA solution and allowed to completely dry under the hood. OVCAR3, SKOV3, and SKOV3ip1 were then seeded in RPMI complete medium without phenol red at a density of 10,000 cells/well in both plates. Cells were resuspended in medium so that the total volume in each well was 100 μl. One plate was cultured for 24 h and the other for 48 h. After 24 or 48 h, cells were incubated for 1 h at 37°C. The standards were prepared and added to the well plates, and 100 μl of reagent was added to each well on the bench. Plates were then incubated for 10 min and then read in a spectrophotometer (SpectraMax M5; Molecular Devices) under luminescence for 1,000 ms according to the manufacturer's instructions.

Amino acid uptake. Ultra-high-performance liquid chromatography (UPLC) was used to assess amino acid uptake and secretion using Waters Aquity UPLC device. Briefly, media samples were deproteinized, and MassTrak Reagent was added to the samples, along with Borate Buffer/NaOH. Samples were then heated and analyzed using the Waters ACQUITY UPLC system with a 2.1 × 150 mm chromatography column maintained at 43°C. Eluents were prepared according to Waters' protocol. MassTrak AAA eluent A concentrate was diluted 1:10 in milliQwater, and MassTrak AAA eluent B was inputted in undiluted form. Flow rate of eluents was 0.4 ml/min, and UV detection was at 260 nm.

OCR measurements. OCR measurements were conducted using a Seahorse XF24 Analyzer. Before the experiment, the Seahorse culture plate was coated with Cell-Tak (BD Biosciences) according to the manufacturer's protocol. Briefly, each well of the Seahorse plate was coated with 50 μl of solution containing Cell-TAK and filtered Sodium Biocarbonate solution, set to dry under the hood, washed with autoclaved water, and set to dry again before use. Tissue culture petri dishes (100-mm dishes) were either coated with Poly-HEMA or uncoated. Cells were seeded at densities of 1.5 million cells per 100-mm petri dish for 48 h. Cells were then trypsinized from the uncoated dishes or collected from the Poly-HEMA-coated dishes. Cell clumps were broken up until single cells were obtained and counted using a hemocytometer. Cells were then seeded in serum-free medium at a density of 50,000 cells/well in a Cell-Tak-coated Seahorse culture plate. Plate was then centrifuged at 450 rpm, centrifuged again at 650 rpm, and then incubated without carbon dioxide. Medium was then changed, and the cells were incubated without carbon dioxide. Prior to the experiment, the Seahorse cartridge was prepared with injections of medium, 2 μg/ml of oligomycin, 2.5 μM of carbonylcyanide-p-trifluoromethoxyphenylhydrazone (FCCP), and 2 μM of antimycin and allowed to calibrate in the machine. The culture plate was then placed in the Seahorse machine to obtain readings.

Wound-healing assay. Ovarian cancer cells were initially seeded in T-75 flasks and cultured for 72 h in either RPMI containing 0 mM or 10 × pyruvate. These cells were then seeded from flasks into 12-well plates in densities that allowed cells to be confluent after 12 h in culture. Assay was performed using low glucose (0.5 mM glucose) RPMI to study specifically the effects of pyruvate on migration. At 12 h after seeding, cell monolayers were scratched using a 200-μl pipet tip, washed, and imaged every 4 h in the same place in each well ≤12 h after seeding. Images were processed using Image J software (National Institutes of Health).

Statistical analysis. Some statistical analysis was performed using Student's two-tailed *t*-test, and these data was reported in all bar graphs as means ± SE. For multiple comparisons, one-way ANOVA with Tukey, Dunn's, or Dunnett's post hoc tests was used for statistical analysis.

RESULTS

Ovarian cancer cells used in metabolic analysis confirmed to be anoikis resistant. Prior to exploring the differences in metabolism between highly invasive and less invasive ovarian cancer cells, live-dead staining was performed to confirm that the differences in metabolism between the cell lines would not be influenced by differences in cell mortality in detached states (Fig. 1*A*). As seen in the figure, a majority of ovarian cancer cells remained viable in nonadherent conditions as in adherent conditions, and mortality was similar in the detached state for all cell lines, confirming first that OVCAR3, SKOV3, and SKOV3ip were anoikis resistant. Furthermore, the metabolic changes observed in the different cell lines, consecutive to the cell detachment, were not affected by cell death.

To further quantify cell viability and confirm that the results were not affected by differences in mortality in detached conditions, a trypan blue exclusion assay was performed. Results showed no significant differences in viability between the different cell lines or between these cells in adherent and nonadherent conditions (Fig. 1*B*). Additionally, this confirms that metabolic findings were not affected significantly by differences in viability between cells in each condition.

Since the goal of our study was to investigate metabolic reprogramming of ovarian cancer cells based on their invasiveness in both adherent and nonadherent cells, we first performed a Matrigel invasion assay to assess invasiveness of the three ovarian cancer cell lines: OVCAR3, SKOV3, and SKOV3ip1. Our results showed that SKOV3 and SKOV3ip1 cancer cells were significantly more invasive than OVCAR3 cells (Fig. 1*C*).

Increase in OCR in highly invasive ovarian cancer cells in detachment. To elucidate the differences in metabolism between highly invasive and less invasive ovarian cancer cells in nonadherent conditions, we first investigated differences in OCR. Although the mitochondria of ovarian cancer cells are known to be competent (18), little is known regarding the differences in metabolism between ovarian cancer cells of different invasive potential and in nonadherent conditions. In contrast to previously known results for adherent cells (3, 25), we found that OCR was significantly higher in nonadherent conditions in the more invasive ovarian cell line SKOV3ip1 than the less invasive cell line OVCAR3 (Fig. 2*A*). Surprisingly, this indicates that these highly invasive ovarian cancer cells may have higher rates of oxidative phosphorylation than less invasive ovarian cancer cells under anoikis conditions, although the reverse is true for adherent conditions. To further examine mitochondrial function of ovarian cancer cells in detachment, we examined the maximum respiratory capacity (Fig. 2*B*). Cells were seeded in Poly-HEMA-coated dishes for 48 h, and OCR was measured after injection of 2.5 μM FCCP. We found that the more invasive ovarian cancer cells (SKOV3 and SKOV3ip1) had significantly higher maximum respiratory capacity (176.96427 ± 7.209774853 and 340.332527 ± 6.518145934 $pmol \cdot min^{-1} \cdot 50{,}000\ cells^{-1}$, respectively) than the less invasive ovarian cancer cell OVCAR3 (90.4147694 ± 12.9885322 $pmol \cdot min^{-1} \cdot 50{,}000\ cells^{-1}$). Furthermore, we examined the mitochondrial reserve capacity or the difference between the OCR measured after injection of 2.5 μM FCCP and basal OCR (Fig. 2*C*). We found that SKOV3ip1 had significantly higher mitochondrial reserve capacity than OVCAR3 (82.53070964 ± 6.24954086 compared with 8.062421829 ± 5.82286257 $pmol \cdot min^{-1} \cdot 50{,}000\ cells^{-1}$). Finally, to complete analysis of the mitochondrial function of the cells, we measured respiratory control ratio (RCR), which indicates the mitochondrial efficiency of ovarian cancer cells in detachment (Fig. 2*D*). We did not find any significant differences in RCR between highly invasive (SKOV3 and

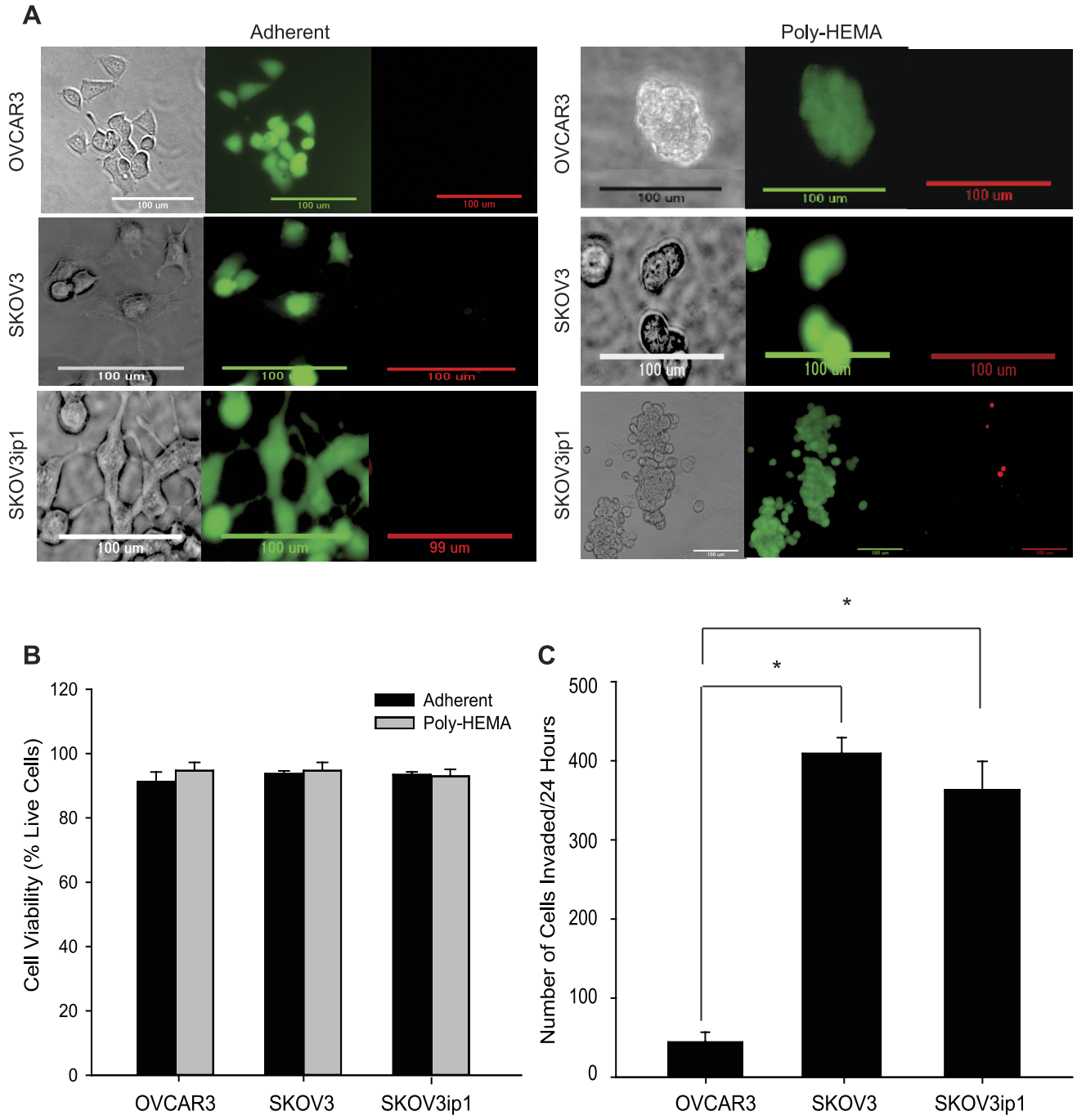

Fig. 1. Cell viability of ovarian cancer cells in 2-dimensional anoikis (anchorage-independent) condition. *A*: calcein AM (green) and ethidium homodimer (red) staining were conducted for OVCAR3, SKOV3, and SKOV3ip1 after 48 h of culture in adherent and nonadherent conditions to confirm that cells remain viable in detached state. *B*: additionally, cell viability was determined for the same cells after 48 h in culture in adherent and nonadherent conditions using trypan blue exclusion assay. Data are expressed as means ± SE; $n = 9$. *C*: a 24-h Matrigel invasion assay was conducted to characterize invasiveness of OVCAR3, SKOV3, and SKOV3ip1. Data are expressed as means ± SE, and 1-way ANOVA with Dunn's post hoc test was used to compare between cell lines in the culture conditions; $n = 4$. *$P < 0.05$. Poly-HEMA, poly(2-hydroxymethacrylate).

SKOV3ip1) and less invasive ovarian cancer cells (OVCAR3), thus indicating that mitochondrial efficiency of these cells was similar.

Higher pyruvate uptake observed in more highly invasive ovarian cancer cells in detachment. Since pyruvate uptake could lead to increased TCA cycle flux and oxygen consumption in cells, we next investigated whether higher oxygen consumption rate under detached conditions correlated with increased pyruvate consumption. We also aimed to investigate the differences in rates of glycolysis between ovarian cancer cell lines of varying invasiveness. To investigate the consumption/secretion rates of various metabolites, we first induced cell detachment conditions using both Poly-HEMA and hydrogel-coated ("low-attachment") culture plates for 24- and 48-h

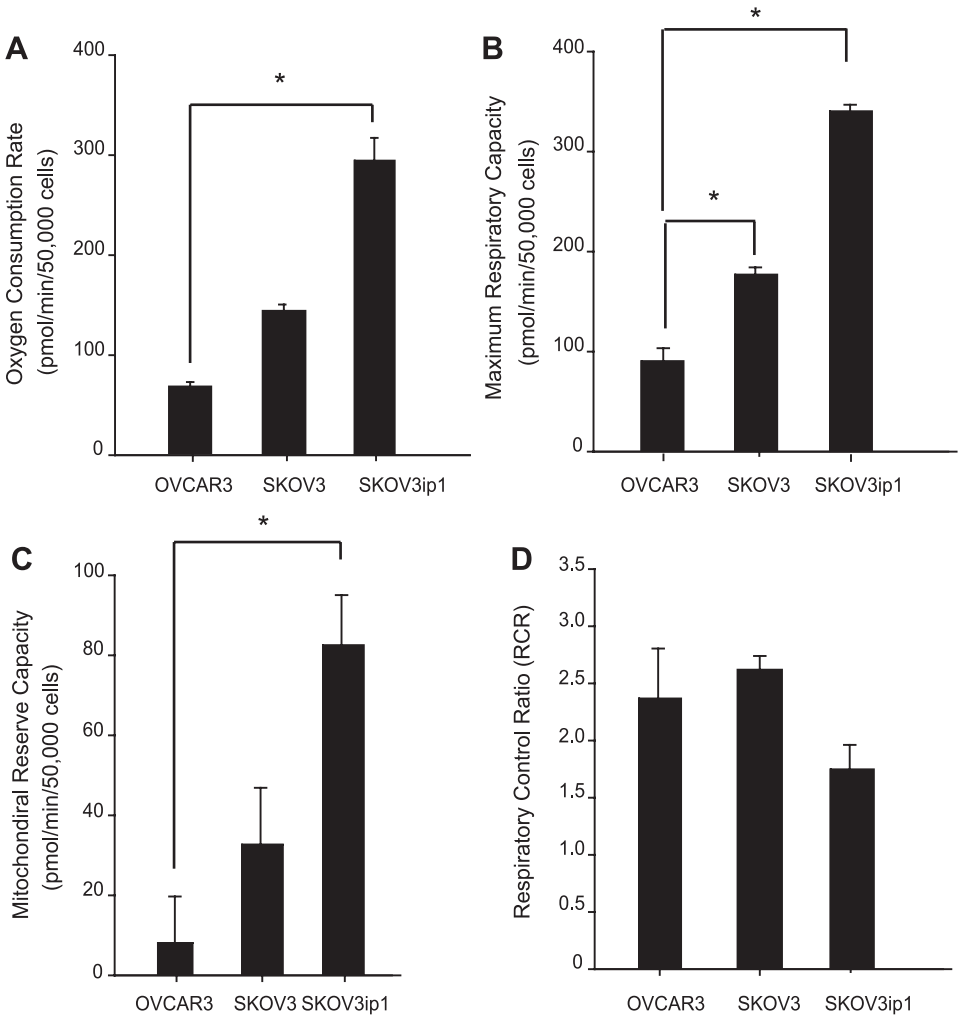

Fig. 2. Effect of nonadherent conditions on ovarian cancer mitochondrial function. Oxygen consumption rate (OCR) of each of these cells cultured in detached conditions (Poly-HEMA) was measured using a Seahorse XF24 Analyzer (*A*), along with maximum respiratory capacity (OCR after injection of 2.5 μM FCCP; *B*), mitochondrial reserve capacity (OCR after injection of 2.5 μM FCCP minus basal OCR; *C*), and respiratory control ratio (*D*). Respiratory control ratio was determined by taking the ratio of basal OCR vs. OCR when cell wells were injected with oligomycin. Data are expressed as means ± SE, and 1-way ANOVA with Dunn's and Dunnett's post hoc tests was used to compare between cell lines in the culture conditions, using OVCAR3 as the control. $*P < 0.05$.

cultures of highly invasive and less invasive ovarian cancer cell lines. Our results show that in almost all of the different experimental conditions the pyruvate consumption was significantly higher in SKOV3 and SKOV3ip1 compared with OVCAR3 cells in detached and attached conditions after 24 and 48 h (Fig. 3, *A–D*). The trends for pyruvate uptake were similar when the cells were cultured in detachment in either Poly-HEMA-coated or hydrogel-coated (low-attachment) plates. When cells were cultured in the low-attachment condition for 24 h, pyruvate consumption was ~2.5-fold higher for SKOV3 and SKOV3ip1 than OVCAR3; adherent SKOV3 and SKOV3ip1 consumed twofold higher pyruvate than OVCAR3 after 24 h (Fig. 3*A*). After 48 h, SKOV3 and SKOV3ip1 cultured in low attachment consumed 2.7- and twofold more pyruvate, respectively, than OVCAR3; adherent SKOV3 and SKOV3ip1 consumed 2.1- and 1.7-fold more pyruvate, respectively, than OVCAR3 (Fig. 3*B*). Similarly, in cells cultured in Poly-HEMA for 24 h, pyruvate consumption was ≈2.7- and 1.8-fold higher in SKOV3 and SKOV3ip1, respectively, than OVCAR3; in the adherent condition, SKOV3 and SKOV3ip1 consumed 1.6- and 1.2-fold more pyruvate, respectively, than OVCAR3 (Fig. 3*C*). When cells were cultured for 48 h in Poly-HEMA-coated plates, SKOV3 and SKOV3ip1 consumed 1.8- and 1.3-fold more pyruvate, respectively, than OVCAR3; adherent SKOV3 and SKOV3ip1 consumed 1.6- and 1.2-fold more pyruvate, respectively, than OVCAR3 (Fig. 3*D*).

Although there were significant differences in pyruvate uptake between cell lines in detached and attached conditions, glucose consumption and lactate secretion in detachment and attachment were not significantly higher for SKOV3 or SKOV3ip1 compared with OVCAR3 after 48 h (Fig. 3, *E–H*). Based on glucose uptake and lactate secretion, our results indicate that rates of glycolysis were not increased significantly in more invasive compared with less invasive ovarian cancer cells in either attachment or detachment.

Amino acid uptake and secretion of highly invasive and less invasive ovarian cancer cells. Next, we decided to determine the correlation between high oxidative phosphorylation and TCA flux with amino acid uptake and secretion of ovarian cancer cells in nonadherent conditions. To investigate amino acid uptake and secretion, ultra-high-performance liquid chromatography (UPLC) was utilized on media collected from cells cultured in attachment or detachment (on Poly-HEMA- or hydrogel-coated plates) for 48 h (Fig. 4). We observed differences in uptake and secretion of amino acids between the cells cultured in different conditions (Fig. 4, *A* and *B*). Interestingly, we observed higher citrulline secretion in the more invasive ovarian cancer cells SKOV3 and SKOV3ip1 than the less

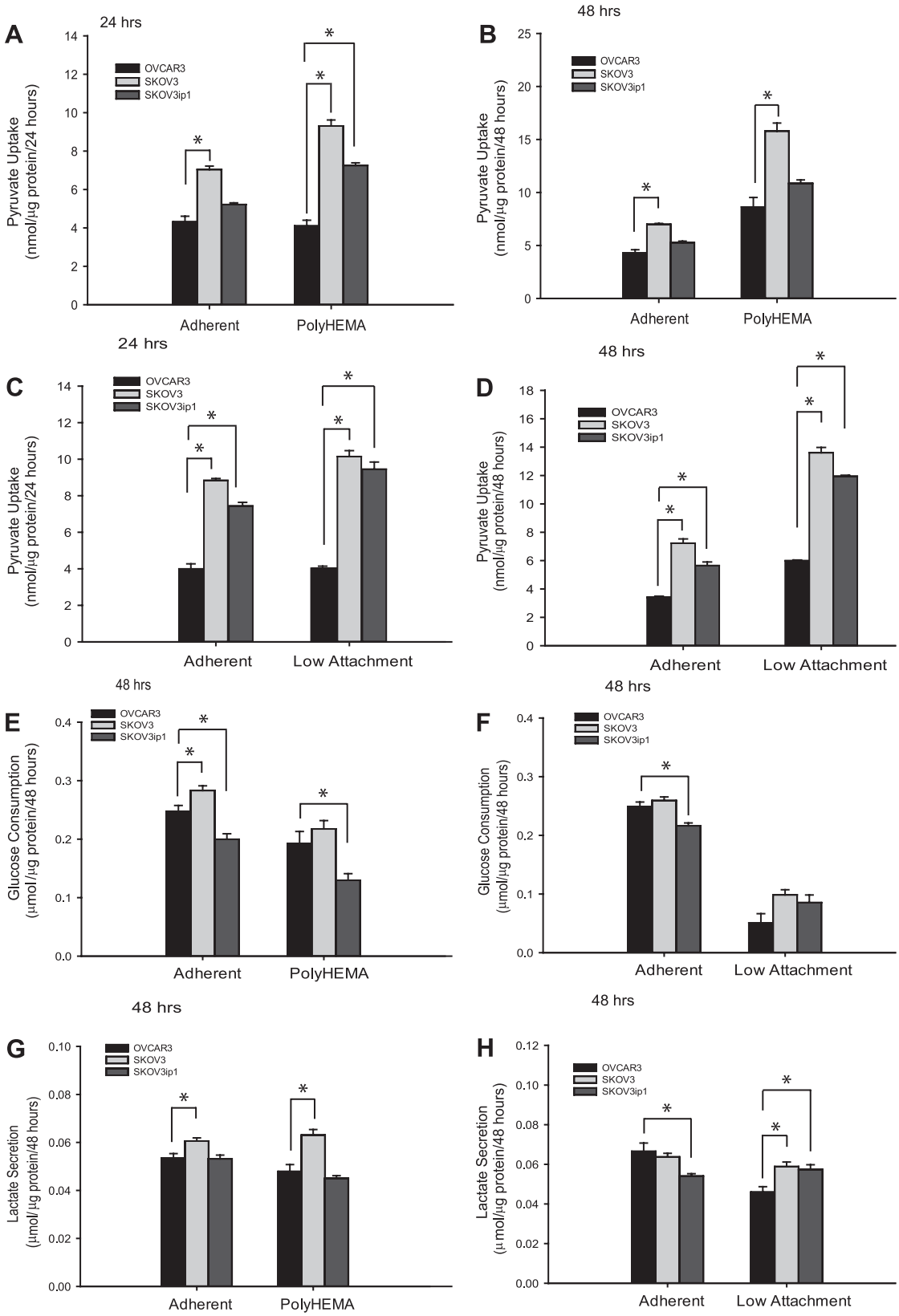

Fig. 3. Effect of nonadherent vs. adherent conditions on ovarian cancer pyruvate uptake, glucose consumption, and lactate secretion. Pyruvate uptake was determined for the ovarian cancer cells in adherent and low-attachment plates (Corning) for 24 (*A*) and 48 h (*B*). In addition, pyruvate uptake was also determined for these cells when cultured in adherent conditions and in Poly-HEMA for 24 (*C*) and 48 h (*D*). Glucose consumption was determined for 48-h cultures in adherent and Poly-HEMA conditions (*E*) and adherent and low-attachment plate conditions (*F*). Similarly, lactate secretion was determined for 48-h cultures in adherent and Poly-HEMA conditions (*G*) and adherent and low-attachment plate conditions (*H*). Data are expressed as means ± SE, and 1-way ANOVA with Dunn's and Dunnett's post hoc tests was used to compare between cell lines in the culture conditions, using OVCAR3 as the control $^*P < 0.05$.

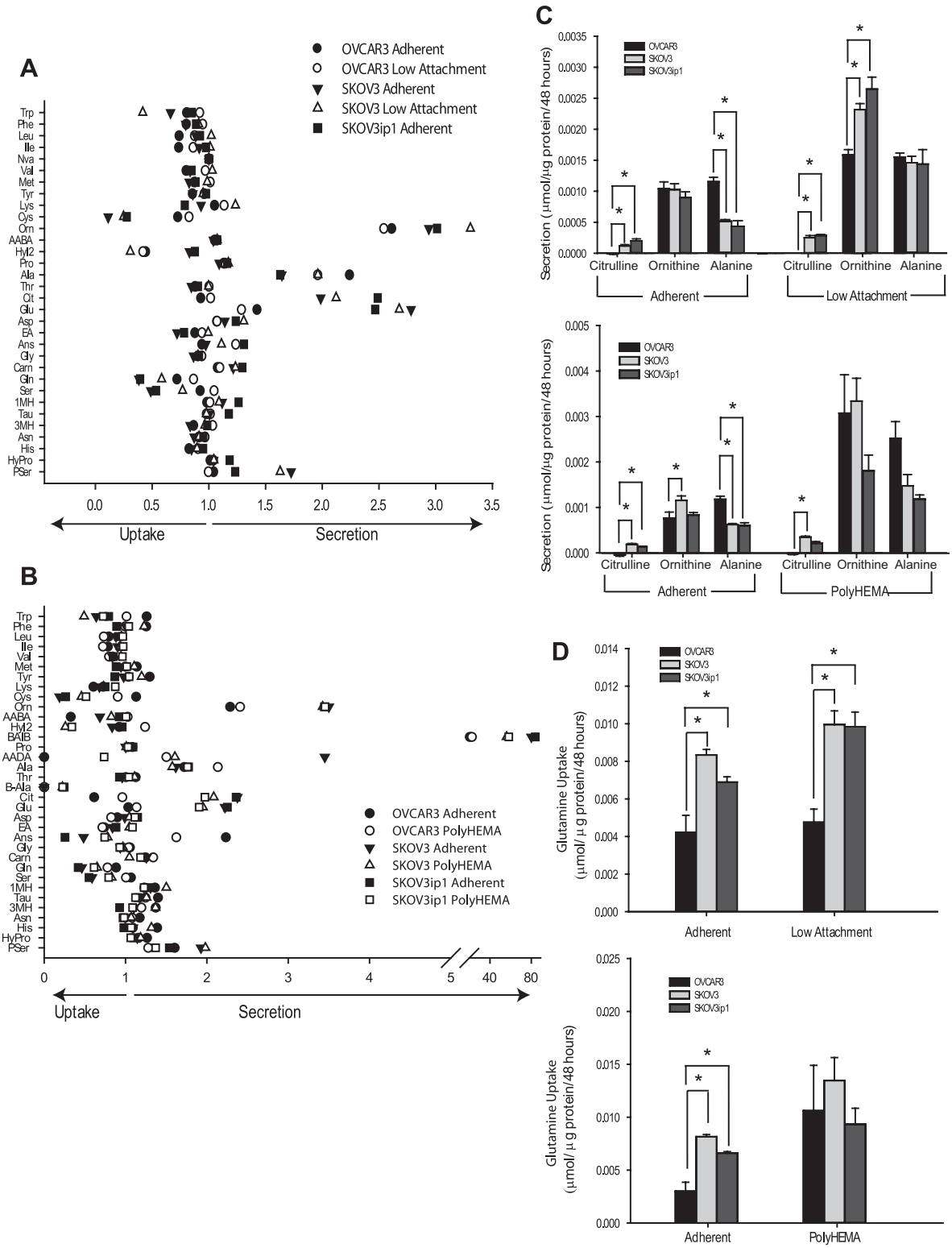

Fig. 4. Secretomics of ovarian cancer cells in adherent vs. nonadherent conditions. Uptake and secretion of amino acids after 48-h culture were determined using ultra-high-performance liquid chromatography. Ratios of amino acid amounts in spent media to original media determined for media in cells cultured in low-attachment and adherent conditions (*A*) and Poly-HEMA and adherent conditions (*B*), as described by Shaham et al. (30). Ratios >1 represent secretion, and ratios <1 represent uptake. *C*: fluxes of secretion for citrulline, alanine, and ornithine were determined for low-attachment, Poly-HEMA, and adherent conditions. *D*: fluxes for glutamine uptake were determined for low-attachment, Poly-HEMA, and adherent conditions. Data in *C* and *D* are expressed as means ± SE, and 1-way ANOVA with Dunn's and Dunnett's post hoc tests was used to compare between cell lines in the culture conditions, using OVCAR3 as the control; $n = 6$. *$P < 0.05$. Pser, phosphoserine; HyPro, hydroxyproline; His, histidine; Asn, asparagine; 3MH, 3-methylhistidine; 1MH, 1-methylhistidine; Ser, serine; Gln, glutamine; Carn, carnosine; Gly, glycine; Ans, anserine; EA, ethanolamine; Asp, aspartate; Glu, glutamate; Cit, citrulline; Thr, threonine; Ala, alanine; Pro, proline; Hyl2, hydroxylysine 2; AABA, α-aminobutyric acid; Orn, ornithine; Cys, cystine; Lys, lysine; Tyr, tyrosine; Met, methionine; Val, valine; Nva, norvaline; Ile, isoleucine; Leu, leucine; Phe, phenylalanine; Trp, tryptophan; B-Ala, B-alanine; AADA, amino acid-N,N-diacetic acid; BAIB, β-aminoisobutyric acid; Tau, taurine.

invasive OVCAR3 in almost all adherent and nonadherent conditions (Fig. 4*C*). This result indicates that detachment of cancer cells affects not only consumption of amino acids but also their catabolism to precursors of nitrogen-containing small molecules.

Glutamine may be increasing TCA cycle flux in highly invasive ovarian cancer cells. Glutamine consumed by cells can enter the TCA cycle and increase the rate of oxidative phosphorylation. Glutamine is first converted to glutamic acid, which is then converted to α-ketoglutarate, a metabolite of the TCA cycle. Therefore, we hypothesized that glutamine was increasing TCA cycle flux in ovarian cancer cells in detachment. We investigated the changes in glutamine uptake rates between the ovarian cancer cells in both attachment and detachment (Poly-HEMA- or hydrogel-coated plates) using UPLC. We observed a significantly higher glutamine uptake in more invasive ovarian cancer cells such as SKOV3 and SKOV3ip1 compared with the less invasive OVCAR3 cells in low attachment (Fig. 4*D*). We also observed a significantly higher glutamine uptake for the more invasive ovarian cancer cells SKOV3 and SKOV3ip1 than less invasive OVCAR3 in attachment (Fig. 4*D*). Thus, glutamine, along with pyruvate, may be a contributor to the higher OCR in more invasive ovarian cancer cells as opposed to less invasive ovarian cancer cells.

Fold changes in uptake and secretion of TCA cycle amino acids. Since pyruvate consumption results indicate that highly invasive ovarian cancer cells have higher TCA cycle flux than less invasive ovarian cancer cells, we hypothesized that there were significant differences in TCA cycle amino acid secretion and uptake between the highly invasive and less invasive cells. A comparison of amino acid secretion and uptake of highly invasive (SKOV3 and SKOV3ip1) ovarian cancer cells and less invasive ovarian cancer cells (OVCAR3) revealed an increased cystine uptake in SKOV3 and SKOV3ip1 compared with OVCAR3 in low-attachment conditions (Figs. 5, *A* and *B*). Fold increase in uptake between the more invasive cell lines SKOV3 and SKOV3ip1 and OVCAR3 in low attachment were 5.3- and 3.9-fold, respectively, and in adherent condition were 3.2- and 2.2-fold, respectively. Since cystine can be converted to pyruvate, the results indicate that uptake of cystine may be further increasing TCA cycle flux through pyruvate and oxidative phosphorylation in highly invasive vs. less invasive ovarian cancer cells. Our results show a fivefold increase in β-amino-isobutyric acid (BAIB) secretion in SKOV3 compared with OVCAR3 (Fig. 5*C*) and a fourfold increase in SKOV3ip1 compared with OVCAR3 (Fig. 5*D*). BAIB secretion has been seen to be elevated in cancer patients compared with healthy controls (34), and our results indicate that it could be a metabolic indicator of more invasive ovarian cancer vs. less invasive ovarian cancer.

In Poly-HEMA, a fold decrease in uptake of the branched-chain amino acids valine, isoleucine, and leucine was observed between SKOV3 and OVCAR3 (Fig. 5*E*) and SKOV3ip1 and OVCAR3 (Fig. 5*F*). These three amino acids can be synthesized from pyruvate, and thus differences in uptake of these amino acids may be linked to differences in pyruvate uptake between these cells in detachment. Our results also revealed a 40-fold decrease in proline secretion in SKOV3 cells compared with OVCAR3 cells in Poly-HEMA and a sevenfold decrease in proline secretion in SKOV3ip1 cells compared with in OVCAR3 cells under detachment conditions (Fig. 5, *G* and *H*). In the adherent condition, a 17.4-fold decrease in proline secretion in SKOV3 cells compared with OVCAR3 and 1.1-fold decrease in proline secretion in SKOV3ip1 cells compared with OVCAR3 was observed. Since proline metabolism is related to oxidative stress (26) and extracellular matrix production, our results suggest that more invasive cancer cells may be subjected to less oxidative stress than less invasive cancer cells and may have reduced extracellular matrix production.

Fold decreases in alanine secretion were also observed between SKOV3 and OVCAR3 (Fig. 5*G*) and SKOV3ip1 and OVCAR3 (Fig. 5*H*). Since alanine can be converted to pyruvate, the differences in alanine secretion can also be linked to the differences in pyruvate uptake between the cells in detachment.

Increased ATP production in highly invasive ovarian cancer cells in detachment. Since pyruvate uptake can create higher flux through the TCA cycle and increase the rate of oxidative phosphorylation and thus lead to increased ATP production, we next investigated whether the more invasive ovarian cancer cells were producing more ATP than the less invasive cancer cell lines. We found that both SKOV3 and SKOV3ip1, the more invasive ovarian cancer cell lines tested, had higher ATP production than OVCAR3 in nonadherent (Poly-HEMA) conditions after both 24 and 48 h (Fig. 6, *A* and *B*). After 24 h, SKOV3 and SKOV3ip1 seeded in Poly-HEMA produced 40 and 45% more ATP, respectively, than OVCAR3. Under adherent conditions, SKOV3ip1 produced 42% more ATP than OVCAR3, whereas SKOV3 did not produce significantly more ATP than OVCAR3 (Fig. 6*A*). After 48 h, SKOV3 and SKOV3ip1 cells seeded in Poly-HEMA produced 55 and 72% more ATP, respectively, than OVCAR3 cells, whereas in adherent conditions SKOV3 and SKOV3ip1 cells produced 33 and 55% more ATP, respectively, than OVCAR3 (Fig. 6*B*). Therefore, ATP production may have an effect on invasiveness of ovarian cancer cells in detachment and attachment and may be linked to increased OCR in more invasive ovarian cancer cells under detached conditions. Notably, the detachment condition has a pronounced effect on ATP generation in more invasive cancer cells.

Increased pyruvate uptake in ovarian cancer cells in spheroidal cultures. Spheroid matrigel cultures have been used by various researchers to simulate anoikis conditions. In matrigel cultures ovarian cancer cells form spheroids, and in long-term cultures, i.e., >7-day cultures, it has been shown that cells in the inner core of the spheroid are detached or loosely attached to the extracellular matrix and thus mimic anoikis conditions (7, 11, 12, 29). We noticed increased glucose uptake in more invasive cells (SKOV3ip1) in spheroid cultures on *day 12* culture compared with *day 6* and no significant differences in lactate secretion (Figs. 7, *A* and *B*). This indicates that glucose consumed by SKOV3ip1 may be increasing flux through the TCA cycle rather than increasing lactate secretion as spheroids grow over 12 days. Remarkably, we observed that highly invasive ovarian cancer cells consumed all of the pyruvate originally in the medium (~1 mM) within 6 days of seeding on Matrigel, with medium being changed and collected every 48 h. This trend was further observed when ovarian cells were cultured in spheroidal conditions in Matrigel over 12 days, with medium changed every 48 h (Fig. 7*C*). Protein analysis of each cell line cultured in Matrigel after 6 and 12 days showed

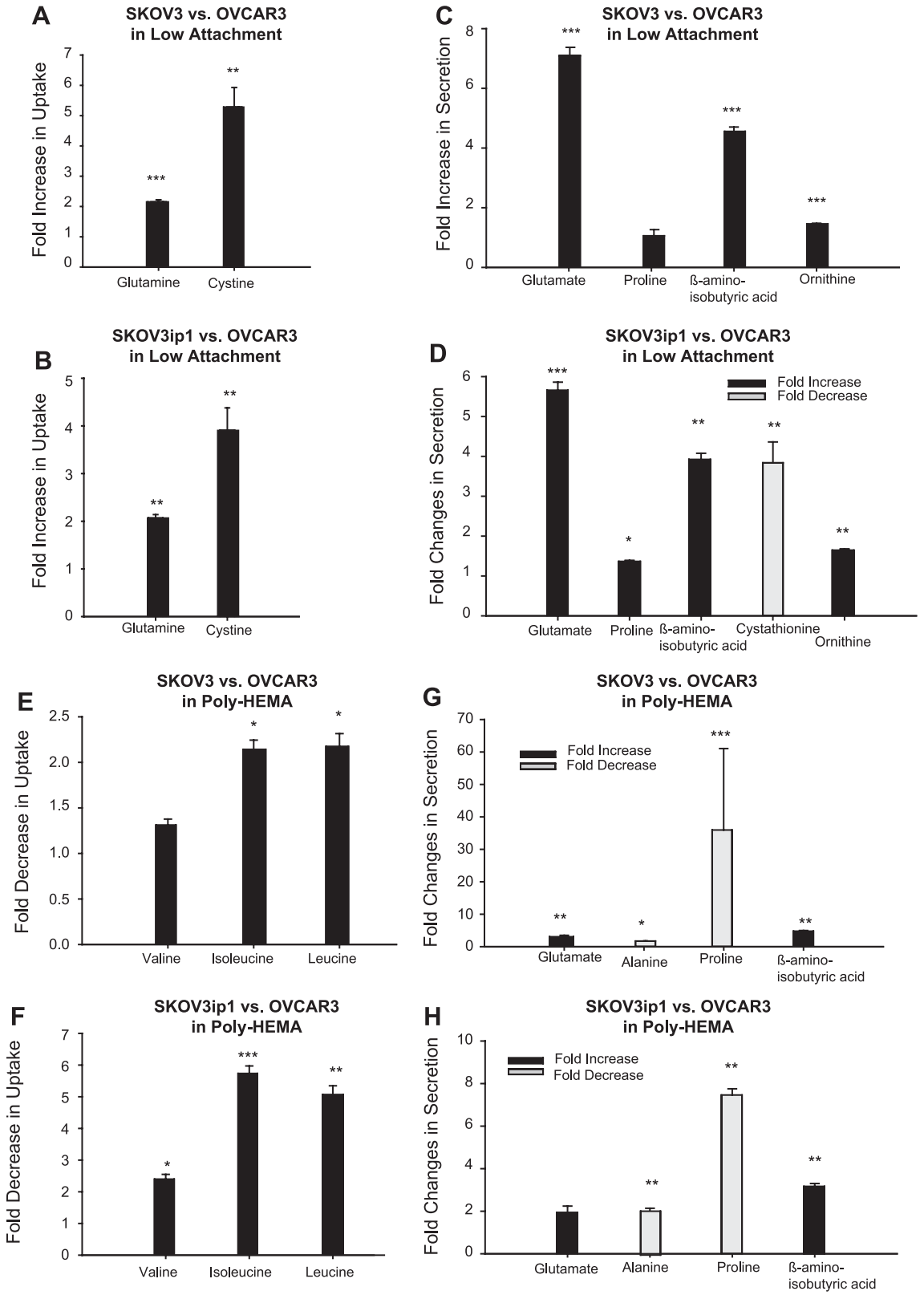

Fig. 5. Effect of ovarian cancer cell invasiveness on secretomics in adherent vs. nonadherent conditions. Uptake and secretion of amino acids of OVCAR3 were compared with that of SKOV3 and SKOV3ip1 by taking a ratio of uptake or secretion of each amino acid for SKOV3 vs. OVCAR3 and SKOV3ip1 vs. OVCAR3 (fold analysis) for low-attachment plate (*A–D*) and Poly-HEMA conditions (*E–H*). Specifically, for low-attachment plate, amino acid uptake ratio of SKOV3 to OVCAR3 (*A*), amino acid uptake ratio of SKOV3ip1 to OVCAR3 (*B*), amino acid secretion ratio of SKOV3 to OVCAR3 (*C*), and amino acid secretion ratio of SKOV3ip1 to OVCAR3 (*D*) are shown. For Poly-HEMA condition, amino acid uptake ratio of SKOV3 to OVCAR3 (*E*), amino acid uptake ratio of SKOV3ip1 to OVCAR3 (*F*), amino acid secretion ratio of SKOV3 to OVCAR3 (*G*), and amino acid secretion ratio of SKOV3ip1 to OVCAR3 (*H*) are shown. Data were expressed as ratio of fluxes of amino acids for each cell line in each condition. Statistics was performed using propagation of error for ratio of 2 averages and *t*-test. Data are expressed as means ± SE; $n > 9$. *$P < 0.05$; **$P < 0.01$; ***$P < 0.001$.

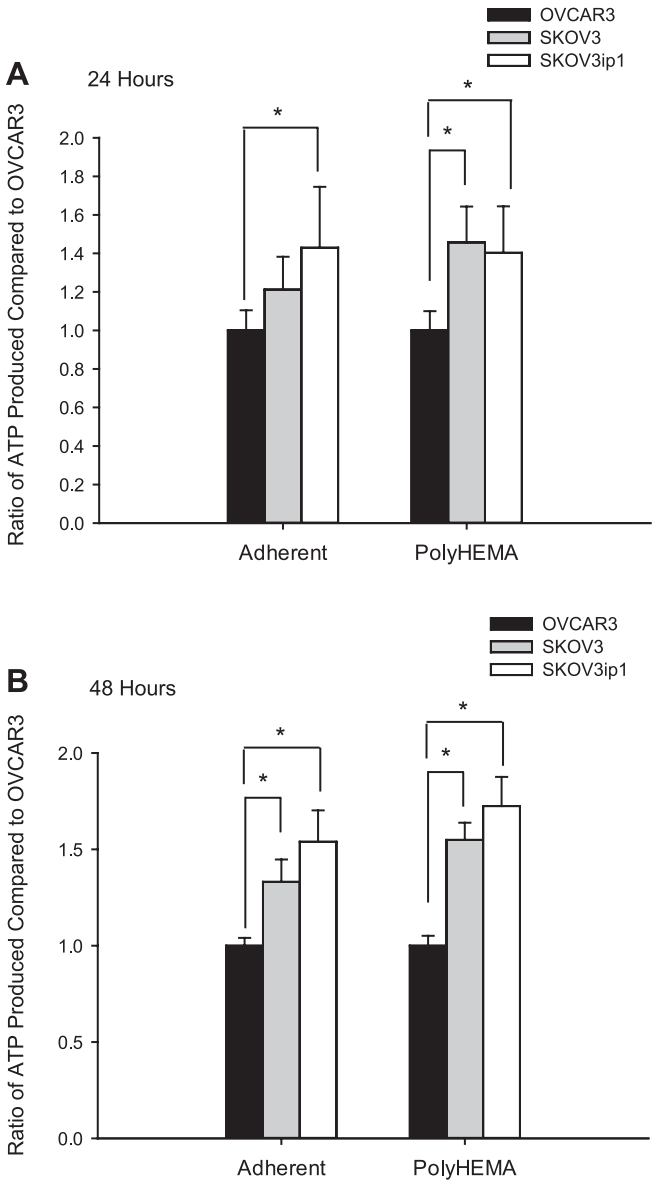

Fig. 6. Effect of invasiveness of ovarian cancer cells on ATP production in attached and detached conditions. ATP production was measured for OVCAR3, SKOV3, and SKOV3ip1 after 24 (*A*) and 48 h (*B*). ATP production was expressed as a ratio of ATP produced by each cell line to the ATP produced by OVCAR3 in both attachment and detachment (Poly-HEMA). Data are expressed as means ± SE, and 1-way ANOVA with Dunn's and Dunnett's post hoc tests were used to compare between cell lines in the culture conditions, using OVCAR3 as the control; $n > 9$. *$P < 0.05$.

that SKOV3ip1 protein was around three times higher on *day 12* vs. *day 6*, indicating that all pyruvate in the media was consumed due to the high rate of cell proliferation of SKOV3ip1 (Fig. 7*D*). When observing the pyruvate content in the medium on *days 6* and *12* of the culture, medium exposed to SKOV3ip1 in Matrigel contained almost no pyruvate, in contrast with OVCAR3 medium (Fig. 7*E*). Even when pyruvate concentration was increased in Matrigel to three times the original concentration, almost no pyruvate was left in the medium after *days 6* and *12* in the SKOV3ip1 Matrigel wells (Fig. 7*F*).

Amino acid uptake and secretion of ovarian cancer cells in spheroidal culture. The higher pyruvate uptake observed above in highly invasive SKOV3ip1 cells vs. less invasive OVCAR3 in spheroidal condition could as a result increase TCA cycle flux in SKOV3ip1 compared with OVCAR3. We hypothesized that TCA cycle flux could be correlated with amino acid uptake and secretion since many amino acids serve as precursors for TCA cycle metabolites. To investigate differences in amino acid uptake and secretion between highly invasive and less invasive ovarian cancer cells in spheroidal culture, UPLC was conducted in medium from OVCAR3 and SKOV3ip1 cultured in Matrigel for 6 and 12 days. Results show large differences in secretion of some amino acids (Fig. 8*A*). Specifically, glutamine uptake rate was higher for SKOV3ip1 than OVCAR3 on *day 6* (Fig. 8*B*). In Matrigel, secretion of citrulline was higher for SKOV3ip1 than OVCAR3 on both *days 6* and *12*, and secretion of alanine was lower for SKOV3ip1 than OVCAR3 on both *days 6* and *12* (Fig. 8*C*). These differences in secretion of nitrogen compounds over the duration of culture suggest differences in amino acids used as precursors of nitrogen-containing small molecules between highly invasive and less invasive ovarian cancer cells and between these cells in spheroidal culture.

Fold changes in uptake and secretion of TCA cycle amino acids in spheroidal culture. A comparison in amino acid uptake between SKOV3ip1 and OVCAR3 in spheroidal culture revealed fold increases in leucine uptake on *day 6* (Fig. 9*A*); in contrast, there was a greater than twofold decrease in uptake of the branched-chain amino acids valine, isoleucine, and leucine on *day 12* (Fig. 9*B*). Since valine, isoleucine, and leucine can be synthesized from pyruvate, the differences in uptake of these amino acids may be linked to differences in pyruvate uptake between *days 6* and *12* of spheroidal culture. Glutamate, proline, alanine, BAIB, and ornithine were secreted by both OVCAR3 and SKOV3ip1 on *days 6* and *12* (Fig. 9, *C* and *D*). We observed a 4.5-fold decrease in alanine secretion between SKOV3ip1 and OVCAR3 on *day 6* and a 1.4-fold decrease on *day 12* (Fig. 9, *C* and *D*). Since alanine can be converted to pyruvate, differences in alanine secretion between SKOV3ip1 and OVCAR3 can be linked to differences in pyruvate uptake observed between these cells in spheroidal culture. Secretion of BAIB is also increased in SKOV3ip1 compared with OVCAR3 when cultured in spheroidal conditions (Fig. 9, *C* and *D*). Since BAIB is a known tumor marker for urinary bladder cancer (13), the increase in BAIB secretion by SKOV3ip1 may be due to its higher invasive potential compared with OVCAR3. Glutamate secretion was also higher in SKOV3ip1 than OVCAR3 on *days 6* and *12* in spheroidal conditions (Fig. 9, *C* and *D*). Since glutamate is a TCA cycle intermediate, fold differences in glutamate secretion between SKOV3ip1 and OVCAR3 in spheroidal conditions may be due to differences in TCA cycle activity.

Pyruvate increases the migratory potential of invasive ovarian cancer cells. Based on our finding that more invasive ovarian cancer cells consumed more pyruvate than less invasive ovarian cancer cells both in two-dimensional detachment (Poly-HEMA and low-attachment conditions) and spheroidal conditions, we investigated whether pyruvate uptake played a role in the invasiveness of ovarian cancer cells. Specifically, we aimed to study the effect of pyruvate on cell migration. Upon studying pyruvate's effect on the migration of OVCAR3

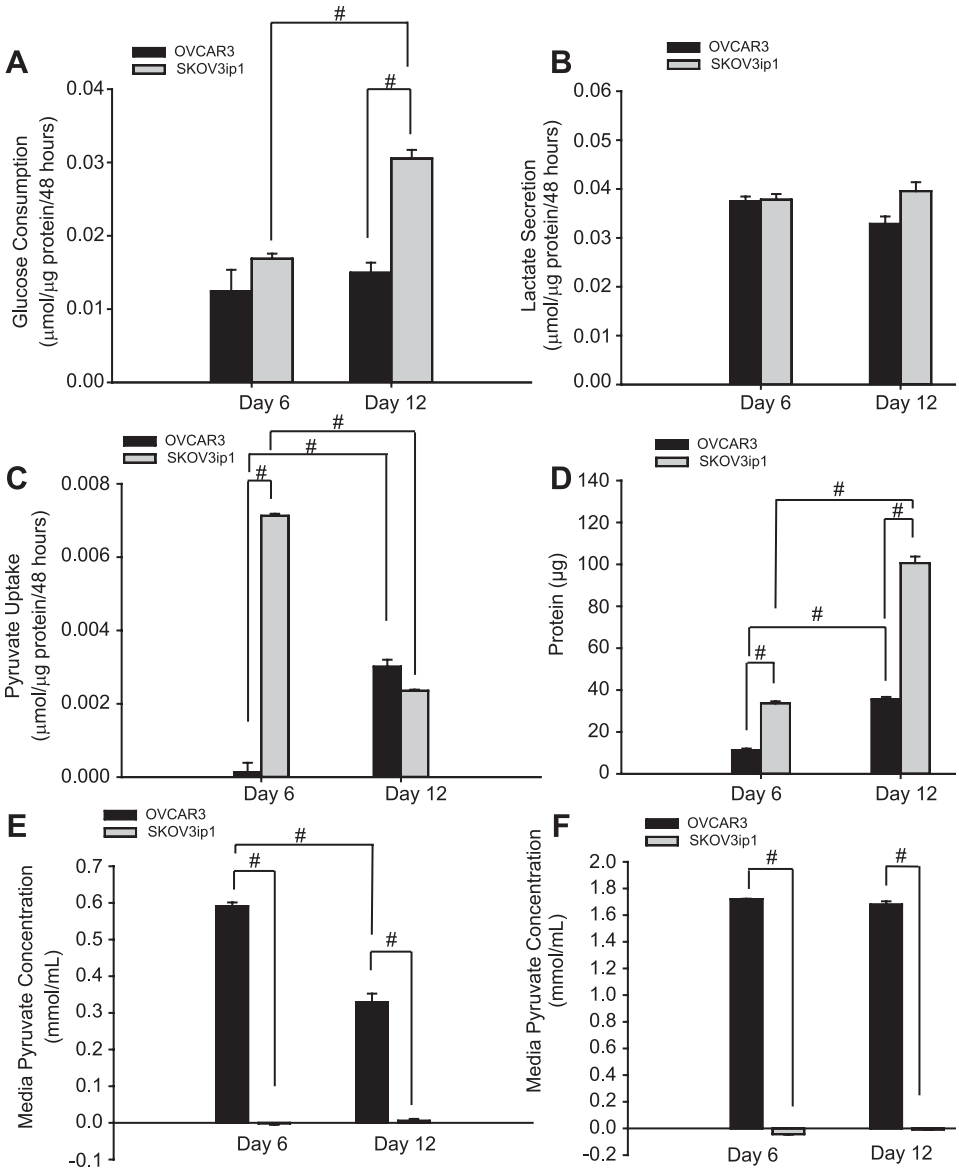

Fig. 7. Effect of spheroidal culture on metabolomic of ovarian cancer cells. Less invasive OVCAR3 and highly invasive SKOV3ip1 cells were seeded in Matrigel for 12 days. Cells were fed with RPMI medium containing 2% Matrigel every other day. Glucose uptake (*A*), lactate secretion (*B*), and pyruvate uptake (*C*) are all expressed in μmol/μg protein. Additionally, protein content was determined for OVCAR3 and SKOV3ip1 after 6 and 12 days in culture (*D*). Concentration of pyruvate left in medium after *days 6* and *12* indicates that SKOV3ip1 consumes all pyruvate in the media even on *day 6*, when cells are cultured in media containing ~1 (*E*) and 3 mM pyruvate (*F*). Data are expressed as means ± SE, and 1-way ANOVA with Tukey post hoc test was used to compare between culture conditions and cell lines; $n = 6$. #$P < 0.05$.

and SKOV3 cells using a wound-healing assay (Figs. 10, *A* and *B*), it was observed that pyruvate contributed to cell migration and that higher concentrations of pyruvate resulted in more migration over the time period of 12 h for SKOV3 but not OVCAR3, indicating that pyruvate may contribute to the motility of these more invasive cancer cells (Fig. 10*B*). We found that cell viability did not decrease for any cell line with the addition of pyruvate vs. no addition of pyruvate (Fig. 10*C*), indicating that migration results are not influenced by differences in cell viability due to pyruvate concentration.

High pyruvate concentration results in significantly larger differences in pyruvate uptake and lactate secretion between ovarian cancer cells in detachment. Since we found that ovarian cancer cells consumed almost all pyruvate in media after 48 h, pyruvate concentration was later increased to 10 times the original concentration in Poly-HEMA culture to further elucidate differences in pyruvate uptake between more highly invasive and less invasive ovarian cancer cell lines 48 h after seeding (Fig. 10*D*). In detachment, SKOV3 and SKOV3ip1 consumed significantly more pyruvate than OVCAR3, respectively, over the 48-h period, whereas in adherent conditions, only SKOV3ip1 consumed significantly more pyruvate than OVCAR3 after 48 h. In addition, the higher pyruvate concentration resulted in higher lactate production for the more invasive ovarian cancer cells vs. the less invasive ovarian cancer cells in detachment and attachment, with increased glucose consumption occurring in highly invasive vs. less invasive ovarian cancer cells in some conditions (Fig. 10, *E* and *F*).

DISCUSSION

In the 1920s, Otto Warburg found that cancer cells have a higher glycolytic rate than normal cells, a phenomenon later named the Warburg effect (35). Ever since Otto Warburg made this finding, researchers have focused on delineating genetic and protein pathways that are responsible for the Warburg effect. Overexpression of glycolysis enzymes has been seen to contribute to this effect in cancer. These include hexokinase

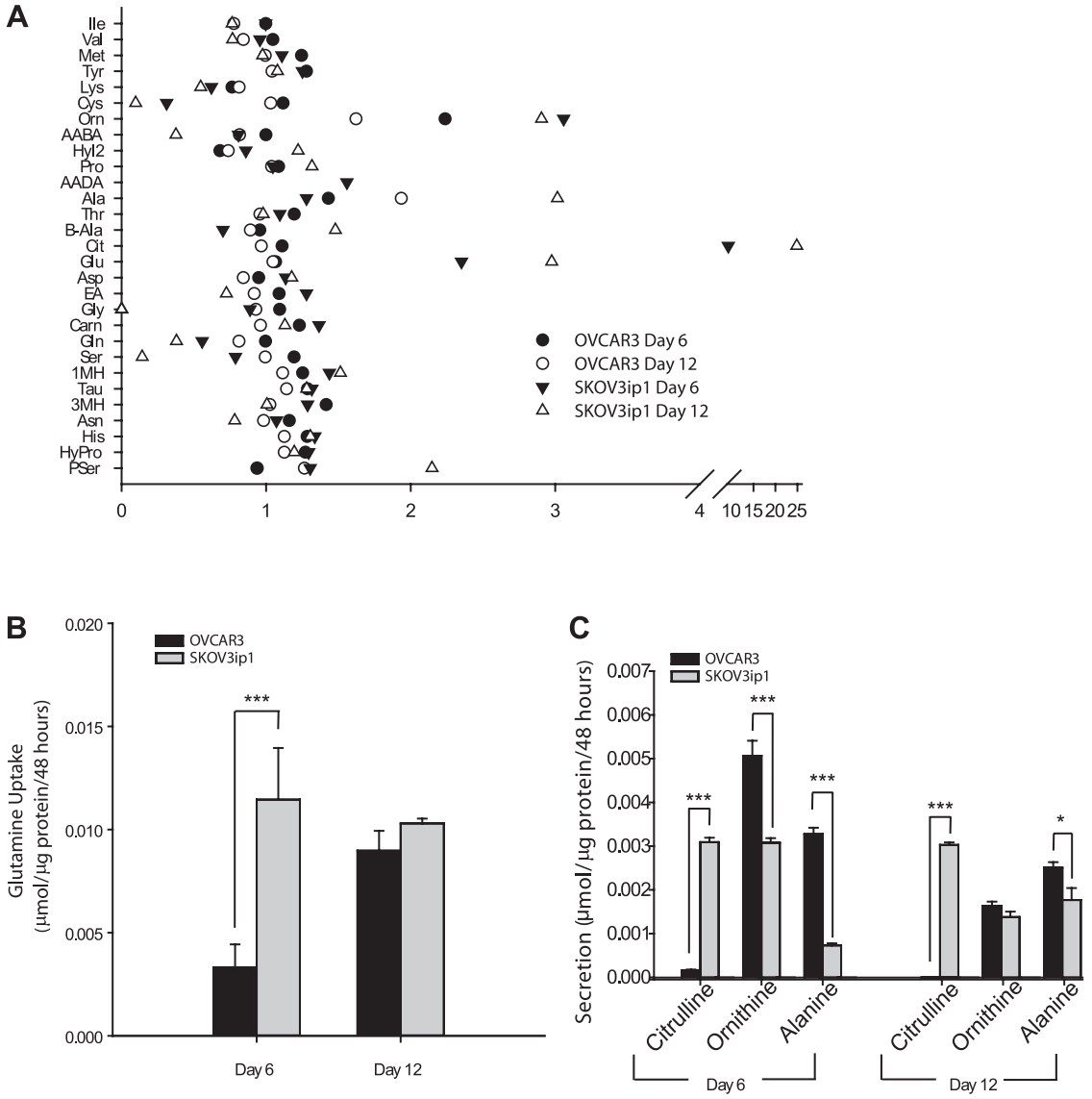

Fig. 8. Secretomics of ovarian cancer cells in spheroidal culture conditions. *A*: uptake and secretion of amino acids were determined using ultra-high-performance chromatography by taking ratio of media to media exposed to cells, as described by Shaham et al. (30). *B* and *C*: fluxes for Gln uptake were determined for SKOV3ip1 and OVCAR3 in spheroidal culture (*B*) as well as for nitrogen compounds (*C*). Data are expressed as means ± SE; $n = 6$. *P < 0.05; ***$P < 0.001$.

and phosphofructokinase-1, which control conversion of glucose to glucose 6-phosphate and conversion of fructose 6-phosphate to fructose 1,6-bisphosphate, respectively (19). Genes for enzymes involved in the glycolytic pathway have also been seen to be overexpressed in several studies (2, 38). Tumor suppressor p53 has also been shown to be involved in increasing rates of glycolysis in cancer cells compared with normal cells (21, 39), as well as HIF-1α (15, 39). Based on these findings, drugs have been created to inhibit glycolysis pathways, including 3-bromopyruvate (9, 16), which inhibits hexokinase, and 2-deoxyglucose (42).

Although strides have been made to clarify the pathways that play a role in cancer cell metabolism, analysis of the overall cancer cell metabolism, including oxidative phosphorylation (OXPHOS) as well as glycolysis, is lacking for ovarian cancer. Studies have shown that OXPHOS is competent in some cancer cells (18, 20, 36). Studying OXPHOS in cancer is important because it may help us better understand the glycolytic pathway and other molecular pathways already known to be involved in cancer malignancy and also can potentially lead us to even more promising molecular targets in addition to glycolysis enzymes. Additionally, the metabolism between highly invasive and less invasive ovarian cancer cells also needs further in-depth exploration, since targeted therapy may rely on this knowledge. SKOV3 has been shown to secrete more vascular endothelisal growth factor A (31) than OVCAR3, and SKOV3ip1 has been categorized as more metastatic than OVCAR3 (27), indicating that SKOV3ip1 and SKOV3 are more highly invasive cell lines than OVCAR3. Additionally, our results in Matrigel invasion confirm that SKOV3 and SKOV3ip1 are more invasive than OVCAR3 (Fig. 1*C*). A study of the differences in metabolism in these ovarian cancer cell lines may potentially lead to more effective targeted ovarian cancer therapies.

In this study, we hypothesized that ovarian cancer cells of varying invasiveness had different metabolic profiles and that

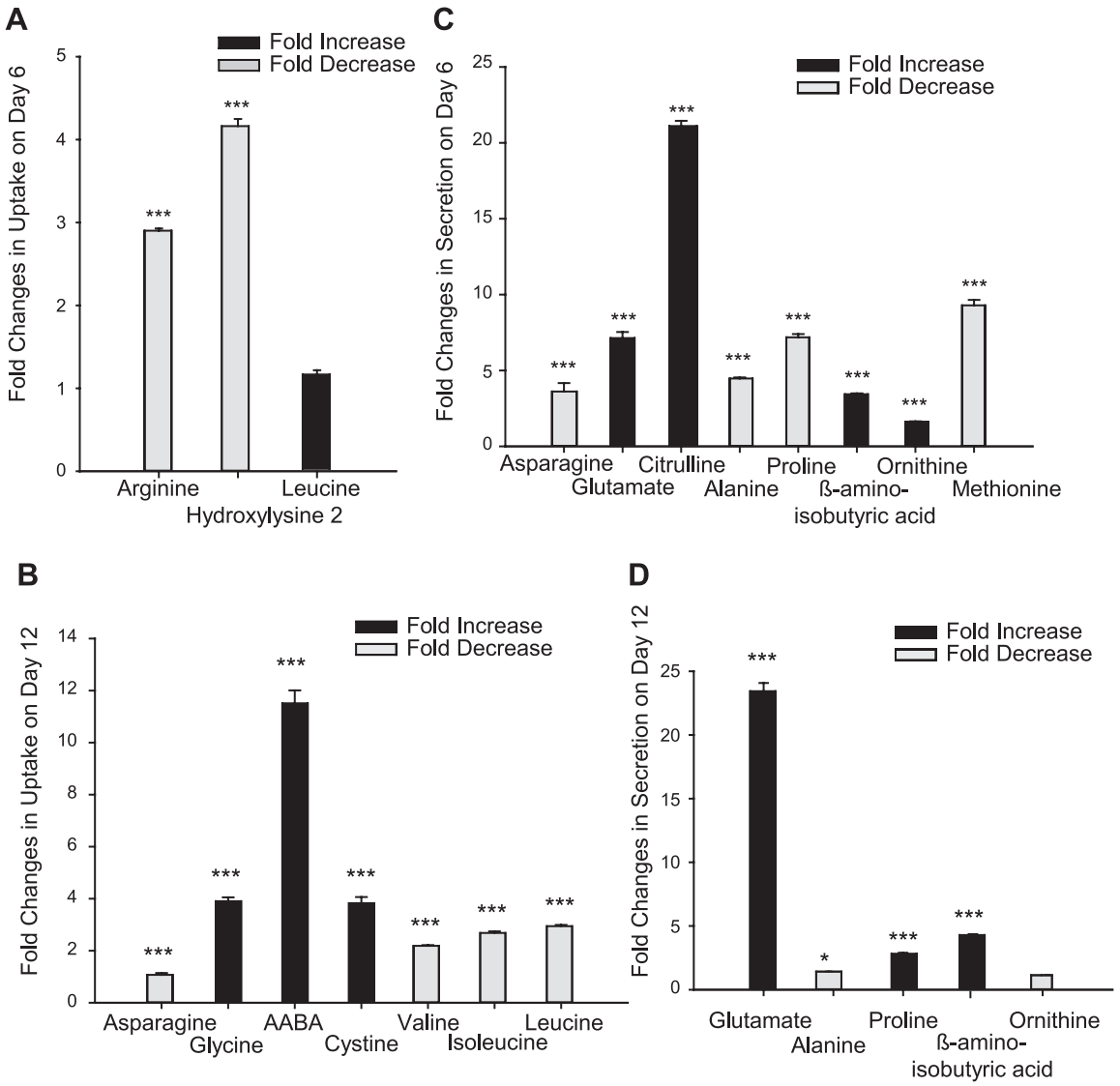

Fig. 9. Effect of ovarian cancer cell invasiveness on secretomics in spheroidal culture. Fold analysis for SKOV3ip1 vs. OVCAR3 was conducted for amino acid uptake on *day 6* (*A*), amino acid uptake on *day 12* (*B*), amino acid secretion on *day 6* (*C*), and amino acid secretion on *day 12* (*D*) of spheroidal culture. Data in *A–D* are expressed as means ± SE; $n > 9$. *$P < 0.05$; ***$P < 0.001$.

their metabolism would be altered in the detached vs. attached state. We have used MFP approach to assess ovarian cancer cell metabolism and have summarized our mechanistic understanding of the metabolism based on our results in Fig. 11. We have shown that OCR is higher in more invasive ovarian cancer SKOV3ip1 cells than less invasive ovarian cancer OVCAR3 cells in detached conditions, as illustrated in the figure. High OCR indicates higher rate of oxidative phosphorylation in the mitochondria. This further indicates that high respiratory capacity may play a role in cancer cell invasiveness.

Additionally, we have found that pyruvate uptake is higher for more invasive ovarian cancer cells than less invasive ovarian cancer cells in detachment. This indicates that pyruvate may be fueling the TCA cycle and may play a role in the increased OCR of more invasive vs. less invasive ovarian cancer cells. One possible mechanism is that pyruvate can be converted into glycerate 2-phosphate in the glycolysis pathway. Pyruvate and serine are uptaken to create hydroxypyruvate, which then is converted to glycerate via NADPH and further into glycerate 2-phosphate through conversion of ADP into ATP (22). In this way, pyruvate may be another metabolite consumed during glycolysis.

From our data, we see that supra-in vitro pyruvate concentrations (~10 mM) lead to larger differences in pyruvate consumption and lactate secretion between highly invasive and less invasive ovarian cancer cells than normal pyruvate concentrations in in vitro cultures (1 mM). This shows that pyruvate concentration can modulate the metabolism of ovarian cancer cells of different invasiveness. Understanding pyruvate metabolism can thus be useful in creating therapies that can be targeted to ovarian cancer of varying invasiveness. Our findings can also be used to create powerful diagnostic tools that can discern highly invasive from less invasive ovarian cancer. Lactate secretion has also been shown to increase in high-grade vs. low-grade prostate cancer tumors using hyper-

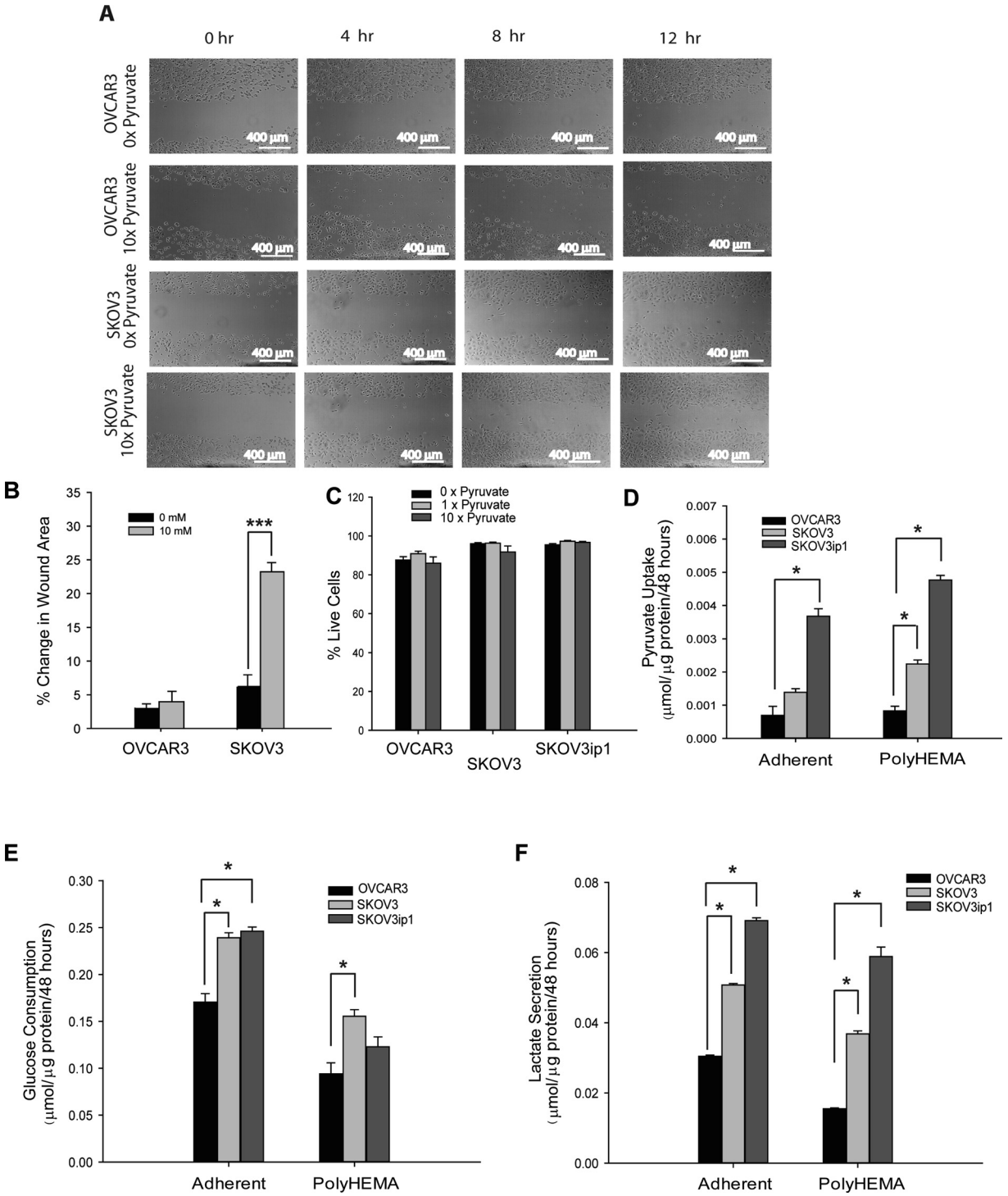

Fig. 10. Effect of pyruvate concentration on migration of highly invasive vs. less invasive ovarian cancer cells. OVCAR3, SKOV3, and SKOV3ip1 were seeded at densities that produced 80–100% confluent monolayers 12 h after seeding. *A*: monolayers were scratched and imaged right after scratching and again every 4 h for ≤12 h. *B*: migration was assessed by creating binary images using Image J and comparing %area taken up by cells in each image. For each condition, the cell migration obtained after 12 h is expressed in percentage of wound area at 0 h. Trypan blue exclusion assay was additionally performed to assess whether addition of pyruvate affected the viability of ovarian cancer cells. *C*: data were reported as %live cells out of all cells in each pyruvate condition. In *B* and *C*, data are expressed as means ± SE; $n = 9$. Pyruvate uptake (*D*), glucose consumption (*E*), and lactate secretion (*F*) were determined after cells were cultured in media containing 10 times the original pyruvate concentration (1 mM). In *D–F*, data are expressed as means ± SE, and 1-way ANOVA with Dunn's and Dunnett's post hoc tests were used to compare between cell lines in the culture conditions, using OVCAR3 as the control; $n = 9$. $^{*}P < 0.05$; $^{***}P < 0.001$.

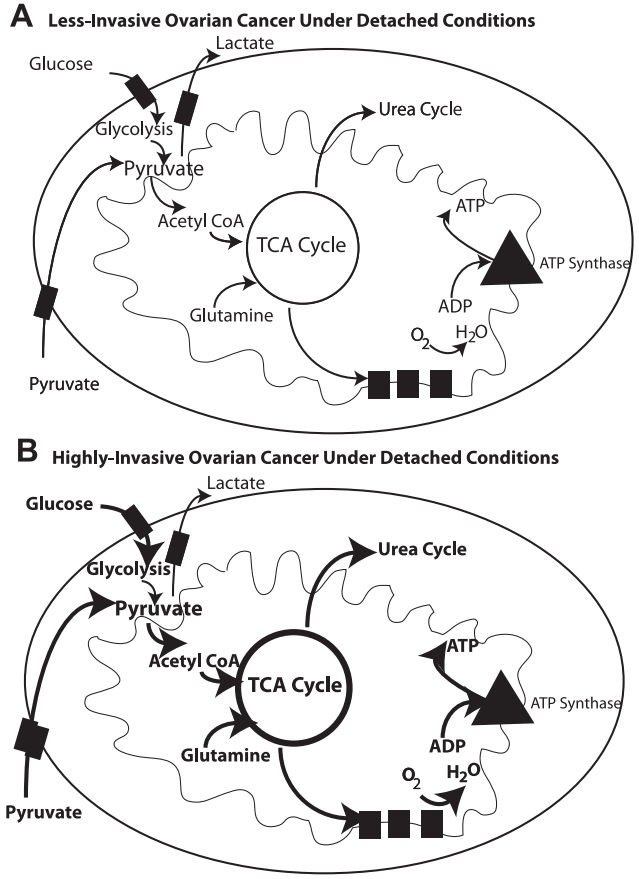

Fig. 11. Mechanistic overview of results. Diagram shows differences in uptake or secretion of metabolites and rates of glycolysis, tricarboxylic acid (TCA) cycle, and electron transport chain between less invasive ovarian cancer cells in detachment (*A*) and highly invasive ovarian cancer cells in detachment (*B*).

polarized [^{13}C]pyruvate, lactate, and alanine analysis (1). Pyruvate uptake can be thus used in addition to lactate secretion in cancer diagnostics.

We also show that pyruvate uptake is higher in the more invasive cell lines (SKOV3ip1) than the less invasive cell line (OVCAR3) in matrigel culture. The three-dimensional culture approach has been used by other researchers to study cancer cells due to its closeness to in vivo tumor morphology (4, 7, 41). Matrigel culture of mammary epithelial cancer cells has been utilized to study lack of luminal clearance and luminal filling that takes place in mammary cancer and the oncogenes that play a role in this observation (7). Other researchers have used three-dimensional approaches to study the reversion between normal and abnormal (cancer) glandular architecture (4, 41). Since our pyruvate results hold for three-dimensional matrigel cultures, this suggests that pyruvate uptake may be higher in more invasive than less invasive ovarian cancer cells in the three-dimensional tumor microenvironment.

Using a secretomics approach, we found that in both spheroidal and two-dimensional cultures, amino acids that take part in the urea cycle, i.e., citrulline, ornithine, and alanine, are secreted in both attached and detached cells. Since citrulline can be produced from mitochondria, which essentially is fueled by pyruvate, citrulline, ornithine, and alanine secretion may indicate high flux through the TCA cycle, which is producing these amino acids at a high rate. In Poly-HEMA, there is a 1.5- to twofold decrease in uptake of the branched-chain amino acids valine, isoleucine, and leucine between SKOV3 and OVCAR3 and a three- to sixfold decrease in uptake of these amino acids between SKOV3ip1 and OVCAR3. Valine, isoleucine, and leucine are part of the pyruvate pathway, and thus uptake of these amino acids may be lower for more invasive ovarian cancer cells, since pyruvate uptake is high. Increased uptake of cystine in low-attachment conditions in highly invasive cells (SKOV3 and SKOV3ip1) compared with less invasive OVCAR3 cells can be due to the fact that cystine is converted into pyruvate and that cancer cells that require more pyruvate may also uptake more cystine. Proline was secreted in all cell lines in Poly-HEMA- and hydrogel-coated plates, which may indicate secretion of matrix to hold cells together in detachment, since the cancer cells in detachment were clustered. Glutamine was also found to be uptaken at a higher rate in more invasive vs. less invasive ovarian cancer cells, which suggests that glutamine may be fueling the TCA cycle, leading to high OCR in more invasive vs. less invasive ovarian cancer cells. Indeed, glutamine has the ability to compensate completely for the absence of glucose and maintain ATP levels (23).

Both pyruvate and lactate have been shown to increase the migration of head and neck cancer cells (10). However, the effect of pyruvate on the migration of cells of other cancers has yet to be researched. Our study is the first to show that pyruvate has the potential to increase migration of ovarian cancer cells and thus possibly increase metastatic potential of these cells. Additionally, our data suggest that pyruvate leads to increased TCA flux and OXPHOS in ovarian cancer cells.

In summary, using metabolomics, we have elucidated the differences in metabolism between highly invasive ovarian cancer cells and less invasive ovarian cancer cells in detachment. Our data show that highly invasive ovarian cancer cells have higher OCR than less invasive ovarian cancer cells in detachment. Additionally, highly invasive ovarian cancer cells uptake significantly more pyruvate than less invasive ovarian cancer cells in detachment, indicating that pyruvate uptake may increase oxidative phosphorylation in ovarian cancer cells. High oxidative phosphorylation in highly invasive vs. less invasive ovarian cancer cells may be responsible for the higher ATP production in highly invasive compared with less invasive ovarian cancer cells in detachment. Amino acid uptake and secretion of ovarian cancer cells in detachment correlate with their pyruvate uptake and increased TCA cycle flux in more invasive ovarian cancer cells. Finally, we have shown that pyruvate may be used by highly invasive ovarian cancer cells to migrate in attached conditions and thus may enhance metastatic potential.

ACKNOWLEDGMENTS

We thank Dr. Anil Sood (M. D. Anderson) for kindly providing us with the SKOV3ip1 cell line for our experiments. We also thank Dr. Juan Marini (Baylor College of Medicine) and Dr. Genevera Allen (Rice University and Baylor College of Medicine) for their help with statistical analysis. We also thank HongYun Zhao and Jordan Harrell for help with revision of the manuscript. Finally, we thank Saket Jha for help with figure preparation.

GRANTS

This work was supported by funding from Rice University to D. Nagrath.

DISCLOSURES

No conflicts of interest, financial or otherwise, are declared by the authors.

AUTHOR CONTRIBUTIONS

C.C. and D.N. did the conception and design of the research; C.C., L.Y., and L.P. performed the experiments; C.C., L.Y., and D.N. analyzed the data; C.C., N.B., and D.N. interpreted the results of the experiments; C.C. prepared the figures; C.C. and D.N. drafted the manuscript; C.C., N.B., and D.N. edited and revised the manuscript; D.N. approved the final version of the manuscript.

REFERENCES

1. **Albers MJ, Bok R, Chen AP, Cunningham CH, Zierhut ML, Zhang VY, Kohler SJ, Tropp J, Hurd RE, Yen YF, Nelson SJ, Vigneron DB, Kurhanewicz J.** Hyperpolarized 13C lactate, pyruvate, and alanine: noninvasive biomarkers for prostate cancer detection and grading. *Cancer Res* 68: 8607–8615, 2008.
2. **Altenberg B, Greulich KO.** Genes of glycolysis are ubiquitously overexpressed in 24 cancer classes. *Genomics* 84: 1014–1020, 2004.
3. **Ayyasamy V, Owens KM, Desouki MM, Liang P, Bakin A, Thangaraj K, Buchsbaum DJ, LoBuglio AF, Singh KK.** Cellular model of Warburg effect identifies tumor promoting function of UCP2 in breast cancer and its suppression by genipin. *PLoS One* 6: e24792, 2011.
4. **Beliveau A, Mott JD, Lo A, Chen EI, Koller AA, Yaswen P, Muschler J, Bissell MJ.** Raf-induced MMP9 disrupts tissue architecture of human breast cells in three-dimensional culture and is necessary for tumor growth in vivo. *Genes Dev* 24: 2800–2811, 2010.

4a. **Bellance N, Pabst L, Allen G, Rossignol R, Nagrath D.** Oncosecretomics coupled to bioenergetics identifies α-amino adipic acid, isoleucine and GABA as potential biomarkers of cancer: Differential expression of c-Myc, Oct1 and KLF4 coordinates metabolic changes. *Biochim Biophys Acta* 1817: 2060–2071, 2012.

5. **Cannistra SA.** Cancer of the ovary. *N Engl J Med* 351: 2519–2529, 2004.
6. **Dai Y, Siemann DW.** Constitutively active c-Met kinase in PC-3 cells is autocrine-independent and can be blocked by the Met kinase inhibitor BMS-777607. *BMC Cancer* 12: 198, 2012.
7. **Debnath J, Mills KR, Collins NL, Reginato MJ, Muthuswamy SK, Brugge JS.** The role of apoptosis in creating and maintaining luminal space within normal and oncogene-expressing mammary acini. *Cell* 111: 29–40, 2002.
8. **Frisch SM, Francis H.** Disruption of epithelial cell-matrix interactions induces apoptosis. *J Cell Biol* 124: 619–626, 1994.
9. **Geschwind JF, Ko YH, Torbenson MS, Magee C, Pedersen PL.** Novel therapy for liver cancer: direct intraarterial injection of a potent inhibitor of ATP production. *Cancer Res* 62: 3909–3913, 2002.
10. **Goetze K, Walenta S, Ksiazkiewicz M, Kunz-Schughart LA, Mueller-Klieser W.** Lactate enhances motility of tumor cells and inhibits monocyte migration and cytokine release. *Int J Oncol* 39: 453–463, 2011.
11. **Grassian AR, Metallo CM, Coloff JL, Stephanopoulos G, Brugge JS.** Erk regulation of pyruvate dehydrogenase flux through PDK4 modulates cell proliferation. *Genes Dev* 25: 1716–1733, 2011.
12. **Grassian AR, Schafer ZT, Brugge JS.** ErbB2 stabilizes epidermal growth factor receptor (EGFR) expression via Erk and Sprouty2 in extracellular matrix-detached cells. *J Biol Chem* 286: 79–90, 2011.
13. **Irving CC.** Biochemically detectable tumor markers in urine of bladder cancer patients. *Cancer Res* 37: 2872–2874, 1977.
14. **Kellenberger LD, Bruin JE, Greenaway J, Campbell NE, Moorehead RA, Holloway AC, Petrik J.** The role of dysregulated glucose metabolism in epithelial ovarian cancer. *J Oncol* 2010: 514310, 2010.
15. **Kim JW, Tchernyshyov I, Semenza GL, Dang CV.** HIF-1-mediated expression of pyruvate dehydrogenase kinase: a metabolic switch required for cellular adaptation to hypoxia. *Cell Metab* 3: 177–185, 2006.
16. **Ko YH, Pedersen PL, Geschwind JF.** Glucose catabolism in the rabbit VX2 tumor model for liver cancer: characterization and targeting hexokinase. *Cancer Lett* 173: 83–91, 2001.
17. **Koonings PP, Campbell K, Mishell DR Jr, Grimes DA.** Relative frequency of primary ovarian neoplasms: a 10-year review. *Obstet Gynecol* 74: 921–926, 1989.
18. **Lim HY, Ho QS, Low J, Choolani M, Wong KP.** Respiratory competent mitochondria in human ovarian and peritoneal cancer. *Mitochondrion* 11: 437–443, 2011.
19. **Marín-Hernández A, Rodríguez-Enríquez S, Vital-González PA, Flores-Rodríguez FL, Macías-Silva M, Sosa-Garrocho M, Moreno-Sánchez R.** Determining and understanding the control of glycolysis in fast-growth tumor cells. Flux control by an over-expressed but strongly product-inhibited hexokinase. *FEBS J* 273: 1975–1988, 2006.
20. **Martinez-Outschoorn UE, Pestell RG, Howell A, Tykocinski ML, Nagajyothi F, Machado FS, Tanowitz HB, Sotgia F, Lisanti MP.** Energy transfer in "parasitic" cancer metabolism: mitochondria are the powerhouse and Achilles' heel of tumor cells. *Cell Cycle* 10: 4208–4216, 2011.
21. **Matoba S, Kang JG, Patino WD, Wragg A, Boehm M, Gavrilova O, Hurley PJ, Bunz F, Hwang PM.** p53 regulates mitochondrial respiration. *Science* 312: 1650–1653, 2006.
22. **Mazurek S.** Pyruvate kinase type M2: a key regulator of the metabolic budget system in tumor cells. *Int J Biochem Cell Biol* 43: 969–980, 2011.

22a. **Nagrath D, Avila-Elchiver M, Berthiaume F, Tilles AW, Messac A, Yarmush ML.** Soft constraints-based multiobjective framework for flux balance analysis. *Metab Eng* 12: 429–445, 2010.

22b. **Nagrath D, Caneba C, Karedath N, Bellance N.** Metabolomics for mitochondrial and cancer studies. *Biochim Biophys Acta* 1807: 650–663, 2011.

23. **Nakashima RA, Paggi MG, Pedersen PL.** Contributions of glycolysis and oxidative phosphorylation to adenosine 5′-triphosphate production in AS-30D hepatoma cells. *Cancer Res* 44: 5702–5706, 1984.
24. **Nomura DK, Lombardi DP, Chang JW, Niessen S, Ward AM, Long JZ, Hoover HH, Cravatt BF.** Monoacylglycerol lipase exerts dual control over endocannabinoid and fatty acid pathways to support prostate cancer. *Chem Biol* 18: 846–856, 2011.
25. **Owens KM, Kulawiec M, Desouki MM, Vanniarajan A, Singh KK.** Impaired OXPHOS complex III in breast cancer. *PLoS One* 6: e23846, 2011.
26. **Phang JM, Liu W, Zabirnyk O.** Proline metabolism and microenvironmental stress. *Annu Rev Nutr* 30: 441–463, 2010.
27. **Rankin EB, Fuh KC, Taylor TE, Krieg AJ, Musser M, Yuan J, Wei K, Kuo CJ, Longacre TA, Giaccia AJ.** AXL is an essential factor and therapeutic target for metastatic ovarian cancer. *Cancer Res* 70: 7570–7579, 2010.
28. **Robey IF, Stephen RM, Brown KS, Baggett BK, Gatenby RA, Gillies RJ.** Regulation of the Warburg effect in early-passage breast cancer cells. *Neoplasia* 10: 745–756, 2008.
29. **Schafer ZT, Grassian AR, Song L, Jiang Z, Gerhart-Hines Z, Irie HY, Gao S, Puigserver P, Brugge JS.** Antioxidant and oncogene rescue of metabolic defects caused by loss of matrix attachment. *Nature* 461: 109–113, 2009.
30. **Shaham O, Slate NG, Goldberger O, Xu Q, Ramanathan A, Souza AL, Clish CB, Sims KB, Mootha VK.** A plasma signature of human mitochondrial disease revealed through metabolic profiling of spent media from cultured muscle cells. *Proc Natl Acad Sci USA* 107: 1571–1575, 2010.
31. **Sher I, Adham SA, Petrik J, Coomber BL.** Autocrine VEGF-A/KDR loop protects epithelial ovarian carcinoma cells from anoikis. *Int J Cancer* 124: 553–561, 2009.
32. **Smit MA, Peeper DS.** Zeb1 is required for TrkB-induced epithelial-mesenchymal transition, anoikis resistance and metastasis. *Oncogene* 30: 3735–3744, 2011.
33. **Sun Q, Chen X, Ma J, Peng H, Wang F, Zha X, Wang Y, Jing Y, Yang H, Chen R, Chang L, Zhang Y, Goto J, Onda H, Chen T, Wang MR, Lu Y, You H, Kwiatkowski D, Zhang H.** Mammalian target of rapamycin up-regulation of pyruvate kinase isoenzyme type M2 is critical for aerobic glycolysis and tumor growth. *Proc Natl Acad Sci USA* 108: 4129–4134, 2011.
34. **van Gennip AH, van Bree-Blom EJ, Abeling NG, van Erven AJ, Voûte PA.** beta-Aminoisobutyric acid as a marker of thymine catabolism in malignancy. *Clin Chim Acta* 165: 365–377, 1987.
35. **Warburg O, Wind F, Negelein E.** The metabolism of tumors in the body. *J Gen Physiol* 8: 519–530, 1927.
36. **Whitaker-Menezes D, Martinez-Outschoorn UE, Flomenberg N, Birbe RC, Witkiewicz AK, Howell A, Pavlides S, Tsirigos A, Ertel A, Pestell RG, Broda P, Minetti C, Lisanti MP, Sotgia F.** Hyperactivation of oxidative mitochondrial metabolism in epithelial cancer cells in situ: visualizing the therapeutic effects of metformin in tumor tissue. *Cell Cycle* 10: 4047–4064, 2011.
37. **Yang W, Xia Y, Ji H, Zheng Y, Liang J, Huang W, Gao X, Aldape K, Lu Z.** Nuclear PKM2 regulates beta-catenin transactivation upon EGFR activation. *Nature* 480: 118–122, 2011.
38. **Yeh CS, Wang JY, Chung FY, Lee SC, Huang MY, Kuo CW, Yang MJ, Lin SR.** Significance of the glycolytic pathway and glycolysis related-genes in tumorigenesis of human colorectal cancers. *Oncol Rep* 19: 81–91, 2008.

39. **Yeung SJ, Pan J, Lee MH.** Roles of p53, MYC and HIF-1 in regulating glycolysis - the seventh hallmark of cancer. *Cell Mol Life Sci* 65: 3981–3999, 2008.
40. **Zha X, Wang F, Wang Y, He S, Jing Y, Wu X, Zhang H.** Lactate dehydrogenase B is critical for hyperactive mTOR-mediated tumorigenesis. *Cancer Res* 71: 13–18, 2011.
41. **Zhang X, Fournier MV, Ware JL, Bissell MJ, Yacoub A, Zehner ZE.** Inhibition of vimentin or beta1 integrin reverts morphology of prostate tumor cells grown in laminin-rich extracellular matrix gels and reduces tumor growth in vivo. *Mol Cancer Ther* 8: 499–508, 2009.
42. **Zhang XD, Deslandes E, Villedieu M, Poulain L, Duval M, Gauduchon P, Schwartz L, Icard P.** Effect of 2-deoxy-D-glucose on various malignant cell lines in vitro. *Anticancer Res* 26: 3561–3566, 2006.
43. **Zhao B, Li L, Wang L, Wang CY, Yu J, Guan KL.** Cell detachment activates the Hippo pathway via cytoskeleton reorganization to induce anoikis. *Genes Dev* 26: 54–68, 2012.